

Structured Information Loss in Network Embeddings

Equivalently-represented graphons, non-invertibility, and downstream tasks

Gabriel Chuang and Augustin Chaintreau

Columbia University

Abstract

We analyze a simple algorithm for network embedding, explicitly characterizing conditions under which the learned representation encodes the graph’s generative model fully, partially, or not at all. In cases where the embedding loses some information (i.e., is not invertible), we describe the equivalence classes of graphons that map to the same embedding, finding that these classes preserve community structure but lose substantial density information. Finally, we show implications for community detection and link prediction. Our results suggest strong limitations on the effectiveness of link prediction based on embeddings alone, and we show common conditions under which naive link prediction adds edges in a disproportionate manner that can either mitigate or exacerbate structural biases.

1 Introduction

Low-dimensional network embeddings (e.g., DeepWalk [1], LINE [2], and many others [3, 4]) are known to be very powerful tools for doing machine learning tasks on graph or network data (for an overview, see [5]). These techniques have shown extremely strong performance in all sorts of tasks including link prediction, community detection, node classification, etc.

However, our theoretical understanding of these methods lags behind their empirical success. This is unsurprising: deep-learning algorithms learn very delicate and complex graph properties from real network data and tasks (prediction, classification, etc.); it is difficult to capture these complex properties in a theoretically-sound generative model, let alone determine whether said properties are faithfully reproduced by any given low-dimensional representation. Furthermore, most network embedding methods rely on minimizing a loss function over subsamples of the graph; it is rare to find analytic characterizations of what these methods converge to.

Recent work has shown theoretical limits on the representation power of arbitrary low-dimensional embeddings [6, 7, 8]. Davison et al [9] show that these representation limits persist even for graphons, a generative model for graphs that can be thought of as probabilistic generalizations of simple graphs. They prove that inner-product-based embeddings “restrict the class of networks for which an informative embedding can be learned, and networks generated from distinct probabilistic models (graphons) can have embeddings which are asymptotically indistinguishable.”

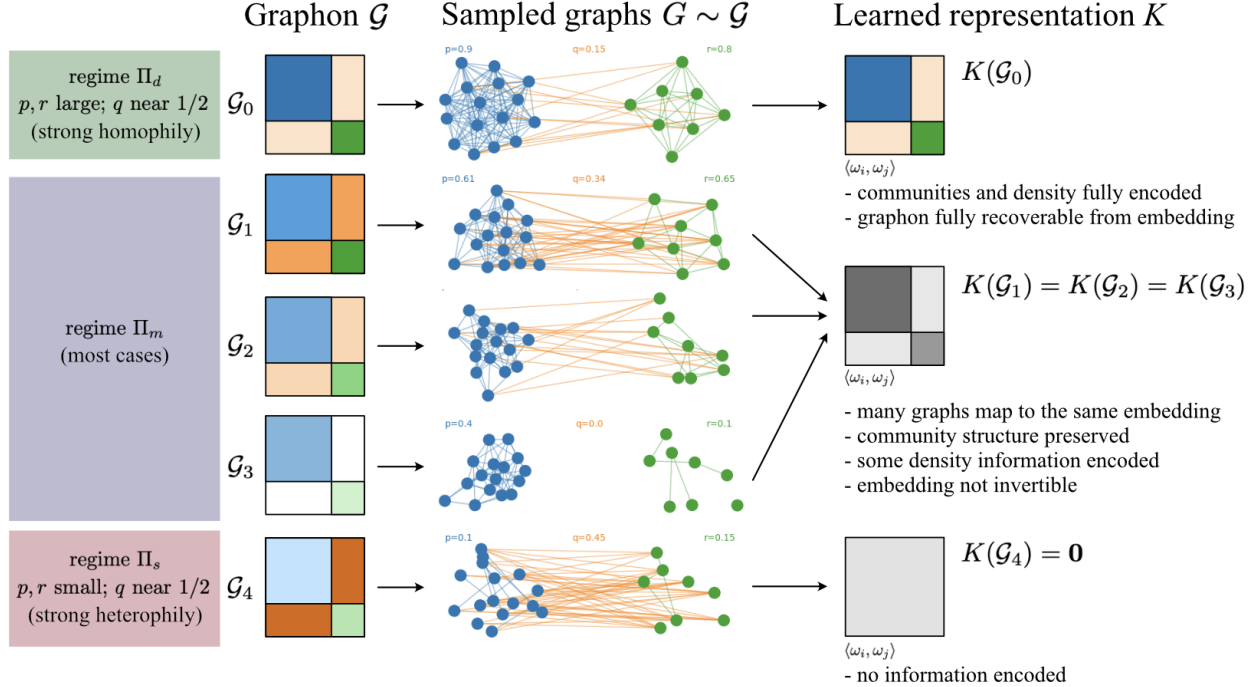


Figure 1: We characterize conditions under which the embedding process encodes full, partial, or no information about the input graphon. In a **dense regime Π_d** , the embedding learns (perfectly) the information of the graphon. In a **sparse regime Π_s** , the embedding is degenerate and loses all information. In **most cases Π_m** , community structure is encoded but only some edge density information is retained; in this regime, many related graphons map to the same representation.

In this work, we ask the following questions:

1. What classes of graphons embed to representations that are fully informative, partially informative, or completely non-informative?
2. When multiple graphons are embedded in an indistinguishable way, how are they related? Can we characterize these equivalence classes?
3. What happens when you perform downstream tasks on these non-unique embeddings?

Like [9], we consider graphs generated using a *graphon*, explicitly choosing to consider learning the generative model rather than a specific instance (i.e., edge set) generated from the model. We focus on a two-community stochastic block model (SBM) graphons. The SBM model captures *homophily* (a well-observed feature of real networks in which nodes tend to be connected to similar nodes [10]), and *heterophily* (in which nodes tend to be connected to dissimilar nodes), as well as majority/minority group structure, while being simple enough to make analysis tractable. We also restrict ourselves to a simple (uniform vertex) sampling scheme.¹

¹More complex random-walk based sampling schemes, like those used in DeepWalk or node2vec, have similar guarantees on unique loss minimizers. We surmise that our results regarding graphon equivalence are likely to extend to this setting; we leave this for future work.

1.1 Contributions.

Our main results are the following (broadly illustrated in Fig. 1):

1. We explicitly characterize conditions under which the embeddings fully, partially, or fail to encode the information of the graph. These conditions depend on the parameters of the SBM, but, interestingly, are independent of the relative sizes of the communities.
 - (a) When the communities are sufficiently dense (many intra-community edges relative to the between-community edges), the embedding preserves (fully) the information of the graphon (i.e., the embedding is invertible). (Theorem 1.1)
 - (b) When the communities are *sparse* relative to the cross-edges, the embedding becomes degenerate (maps all nodes to the zero vector, or similar). (Theorem 1.2a)
 - (c) Otherwise, the embedding preserves community structure and some edge-density information. In this regime, an equivalence class of linearly-related graphons have identical embeddings. (Theorem 1.2b, 1.3)
2. In cases where the embedding is not one-to-one, we describe exactly the equivalence classes of graphons that map to the same embedding. Notably, these equivalence classes are very “wide”: very different graphs are embedded to identical representations.
3. These have very important consequences for downstream tasks that rely on the embeddings. In particular, community detection is robust in most parameter regimes; on the other hand, tasks like link prediction or graph reconstruction are only robust in a narrow dense-communities regime because the representations lose significant density information. We also describe consequences for the preferential treatment of sparser/smaller communities and other fairness considerations.

2 Background

2.1 Limitations of low-dimensional graph representations

For a survey of recent work on the limitations of graph embeddings, see [6]. For example, [7] show that low-dimensional inner product based embeddings cannot encode both low degree and high clustering coefficient, and [8] shows that neighborhood preservation in arbitrary metric spaces requires very high embedding dimension. [11] develop a method for approximately *inverting* graph embeddings (that is, finding a graph that maps to a given embedding); they find that both global properties (like triangle density) and local properties (like existence of a particular edge) are often lost, but that the community structure is typically preserved and sometimes even enhanced (i.e., the conductance within the community is decreased). Our work provides a potential explanation for this behavior, by characterizing a family of SBM graphs (of varying community density) that are embedded identically.

A recent paper by Davison et al [9] develops methods for showing the limiting distributions of embeddings that are based on minimizing subsampling-based losses on exchangeable graphs (i.e., graphons). They show that unique loss-minimizing embeddings exist (up to symmetry), and prove statistical rates of convergence to these asymptotic minimizers. They show a simple case where an inner-product-based embedding is non-invertible, and prove that using an alternative indefinite inner product resolves these invertibility problems in a way that the standard inner product cannot.

However, the standard inner product is likely to remain prevalent in practice, so their work leaves unanswered many important questions about the behavior of representations in practice, which we explore in this work.

In parallel, there has been substantial work on theoretical expressivity limits on Graph Neural Networks (GNNs), a different method for learning graph embeddings (for example, see [12]). GNNs have a fundamentally different objective, often being trained for a particular task (unlike embeddings, which are multi-purpose and task-agnostic), and have a different structure that leads to expressivity results that are orthogonal to what we describe here.

2.2 Graphons

Graphons were originally introduced by Lovasz [13] to describe convergent dense graph limits, and are extensively used throughout the networks literature as a generative model of (exchangeable) graphs [14] due to the Aldous-Hoover theorem [15]. Recently, graphons have also become a foundational model in domains such as economics and network games [16, 17].

A *graphon* is a generative model for graphs which generalizes Erdos-Renyi graphs, consisting of a function $W : [0, 1]^2 \mapsto [0, 1]$. A graph can be sampled from the graphon by first sampling n vertices with latent features $\lambda_i \sim \text{Unif}([0, 1])$, and then adding edges independently, where edge (i, j) is sampled with probability $W(\lambda_i, \lambda_j)$.

In this work, we focus on *Stochastic Block Model (SBM)* graphons, which are a long-studied generative model for networks that capture community structure and homophily (e.g., [18, 19]). A n -block SBM graphon is a symmetric block-constant graphon with $n \times n$ blocks. They can be interpreted as having n “communities” of nodes, where the probability that an edge (i, j) exists depends only on which communities i and j belong to. For example, the graphon below (which can be represented by the block matrix on the right) is a two-block SBM, with a large community (70% of nodes) with strong homophily (90% edge-density within the community), a smaller community (30% of nodes) with weak homophily (40% edge density), and sparse between-community connectivity.

$$W(\lambda_i, \lambda_j) = \begin{cases} 0.9 & \lambda_i \in [0, 0.7], \lambda_j \in [0, 0.7] \\ 0.4 & \lambda_i \in (0.7, 1], \lambda_j \in (0.7, 1] \\ 0.1 & \text{otherwise} \end{cases} \quad W = \begin{matrix} & \begin{matrix} 0.7 & 0.3 \end{matrix} \\ \begin{matrix} 0.7 \\ 0.3 \end{matrix} & \begin{bmatrix} 0.9 & 0.1 \\ 0.1 & 0.4 \end{bmatrix} \end{matrix}$$

3 Setup

Throughout, we will use $\sigma(x) = \frac{e^x}{1+e^x}$ to denote the standard logistic function and $\sigma^{-1}(x) = \ln(x) - \ln(1 - x)$ to denote its inverse (the logit function). We use $\langle \cdot, \cdot \rangle$ to denote the standard inner product. We write $o_p(1)$ to denote a sequence of random variables that converges to zero in probability.

3.1 Generic node embedding algorithm

Following [9], we consider the general node embedding algorithm shown in Algorithm 1 for some stochastic sampling scheme of a graph S and edge-wise loss function ℓ that depends on the inner

Algorithm 1 Node embedding for a graphon (generic)

Parameters: Graph subsampling scheme S , loss function ℓ

Input: Graphon \mathcal{G} , embedding dimension d , graph size n

Output: vertex representations $\omega_i \in \mathbb{R}^d : i = 1, 2, \dots, |V|$

- 1: Initialize $w_i \in \mathbb{R}^d$ in some way (e.g., uniform)
- 2: **while** convergence not reached **do**
- 3: Sample graph $G \sim_n \mathcal{G}$ with $G = (V, E), |V| = n$.
- 4: Sample subgraph $s = S(G)$
- 5: Compute loss $\ell(s, (\omega_1, \dots, \omega_{|V|}))$ (e.g., $\ell = \sum_{(i,j) \in S} \ell_{\text{pairwise}}(\langle \omega_i, \omega_j \rangle, S[i, j])$)
- 6: Perform a gradient update to $\{\omega_1, \dots, \omega_n\}$.
- 7: **end while**

products of embeddings. Many network embedding algorithms (e.g., node2vec, DeepWalk) are instantiations of this structure, mainly with variations in the sampling scheme S .

We study the generic algorithm with the following choice of sampling scheme, loss function, and set of graphons:

Definition 1 (Uniform Vertex Sampling). *The graph subsampling scheme S uniformly selects k vertices of G and returns the induced subgraph.*

Definition 2 (Cross-Entropy Loss). ℓ_{pairwise} is the cross-entropy loss $\ell(y, x) = -x \log(\sigma(y)) - (1 - x) \log(1 - \sigma(y))$

Definition 3 (2-block Stochastic Block Model). *The graphon \mathcal{G} is a 2-block SBM with parameters $(a, (p, q, r))$: that is, it takes the following form:*²

$$W(\lambda_i, \lambda_j) = \begin{cases} p & \lambda_i \in [0, a], \lambda_j \in [0, a] \\ r & \lambda_i \in (a, 1], \lambda_j \in (a, 1] \\ q & \text{otherwise} \end{cases} \quad W = \begin{array}{|c|c|} \hline a & 1 - a \\ \hline a & \begin{array}{|c|c|} \hline p & q \\ \hline q & r \\ \hline \end{array} \\ \hline 1 - a & \begin{array}{|c|c|} \hline q & r \\ \hline \end{array} \\ \hline \end{array}$$

3.2 The limiting embedding and $K(\mathcal{G})$

Davison et al [9] show that the generic procedure (Alg. 1) minimizes the empirical risk function

$$\mathcal{R}_n(\omega_1, \dots, \omega_n) = \sum_{i,j \in [n], i \neq j} \Pr((i, j) \in S(G_n) \mid G_n) \ell_{\text{pairwise}}(\langle \omega_i, \omega_j \rangle, a_{ij}). \quad (1)$$

Furthermore, they show that the minimizers of the empirical risk (1) are unique up to symmetry/rotation, i.e., that, for a given graph \mathcal{G}_n and sampling scheme S , there exists a unique inner-product matrix $K(\mathcal{G}) \in \mathbb{R}^{n \times n}$ such that all loss-minimizing $\hat{\omega}_i$ satisfy

$$\frac{1}{n^2} \sum_{i,j} |\langle \hat{\omega}_i, \hat{\omega}_j \rangle - K(\mathcal{G})_{i,j}| = o_p(1).$$

²Without loss of generality, we let $a \geq \frac{1}{2}$.

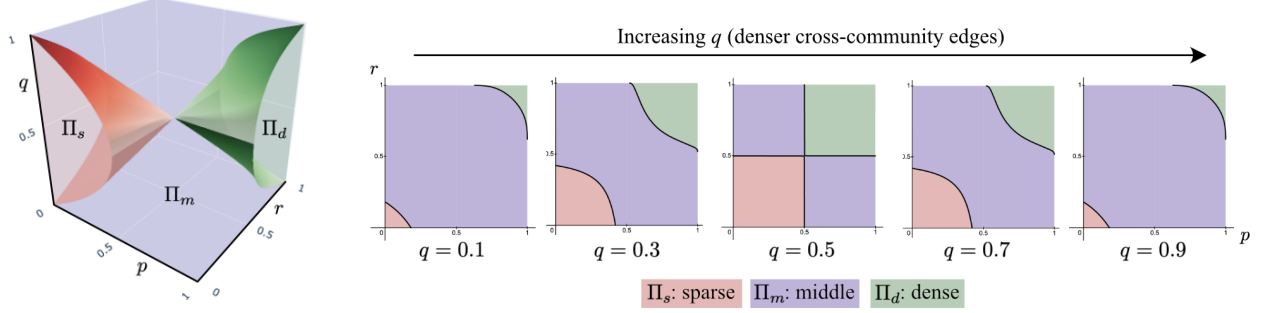


Figure 2: Regions of parameter space in which `none`, `some`, and `all` of the information of the graphon is preserved in the embedding.

In a sense, $K(\mathcal{G})$ is “the embedding of \mathcal{G} ” just as much as $\{\omega_i\}_{i \in [n]}$ is: since training depends only on the pairwise inner products, the unique minimizer is fully captured by the matrix of inner products. Therefore, we seek to analytically characterize the inner-product matrices $K(\mathcal{G})$ of these limiting embeddings, find closed forms (where they exist) and determine what families of graphons have the same K .

4 Results

4.1 Characterizing parameter regimes by information loss

We partition the (p, q, r) parameter space into three regions, depicted in Fig. 2:

- Π_d (“dense”): $p \geq \frac{1}{2}, r \geq \frac{1}{2}$, and $\sigma^{-1}(q)^2 \leq \sigma^{-1}(p)\sigma^{-1}(r)$;
- Π_s (“sparse”): $p \leq \frac{1}{2}, r \leq \frac{1}{2}$, and $(1/2 - q)^2 \leq (1/2 - p)(1/2 - r)$;
- Π_m (“middle”): $[0, 1]^3 \setminus \Pi_d \setminus \Pi_s$.

Our results can be summarized as follows (with formal statement in Theorem 1):

Dense communities Π_d (Theorem 1.1): When the two communities are sufficiently dense (many intra-community edges relative to the between-community edges), the embedding preserves (fully) the information of the graphon (i.e., the embedding is invertible). This occurs when $p, r \geq \frac{1}{2}$ and $\sigma^{-1}(q)^2 < \sigma^{-1}(p)\sigma^{-1}(r)$, which we denote as parameter region Π_d .

Sparse/heterophilic communities Π_s (Theorem 1.2): When the two communities are *sparse* relative to the cross-edges, the embedding becomes degenerate (maps all nodes to the zero vector, or similar). This occurs when $p, r \leq 1/2$ and $(1/2 - q)^2 \leq (1/2 - p)(1/2 - r)$, which we denote as parameter region Π_s . Intuitively, the cross-community (heterophilic) edges overpower the intra-community (homophilic) edges, so both the community structure and the edge density information is lost by the embedding.

Intermediate region Π_m (Theorem 1.3): Otherwise, the embedding preserves only partial information: the mapping of nodes to communities is encoded, but the densities of the communities are only encoded in a relative way. This lossy embedding also implies that, for each embedding, there is an equivalence class of graphons that all map to it.

We formally state this result as follows.

Theorem 1 (Embedding Limit Regimes). *Suppose the graphon \mathcal{G} is a 2-block SBM($a, (p, q, r)$), and let ω_i be the embeddings learned by Algorithm 1 at convergence. Then, the inner product matrix of the embeddings $K(\mathcal{G}) \in \mathbb{R}^{n \times n}$ is a block-constant matrix:*

$$K(\mathcal{G}) = \begin{bmatrix} K_1 \mathbf{1}_{an \times an} & K_2 \mathbf{1}_{an \times (1-a)n} \\ K_2 \mathbf{1}_{(1-a)n \times an} & K_3 \mathbf{1}_{(1-a)n \times (1-a)n} \end{bmatrix},$$

where the values of $K_i \in \mathbb{R}$ depend on a, p, q, r as follows:

1. If $p, r \geq 1/2$ and $\sigma^{-1}(q)^2 < \sigma^{-1}(p)\sigma^{-1}(r)$, then $K_1 = \sigma^{-1}(p), K_2 = \sigma^{-1}(q), K_3 = \sigma^{-1}(r)$.
2. Otherwise, if $p, r \leq 1/2$ and $(1/2 - q)^2 \leq (1/2 - p)(1/2 - r)$, then $K_1 = K_2 = K_3 = 0$.
3. Otherwise,

$$K_2 = \begin{cases} -\sqrt{K_1 K_3} & \text{if } q \leq \frac{1}{2} \\ +\sqrt{K_1 K_3} & \text{if } q > \frac{1}{2} \end{cases},$$

with K_1, K_3 satisfying:

$$\begin{aligned} a^2(\sigma(K_1) - p) - \mu K_3 &= 0 \\ (1-a)^2(\sigma(K_3) - r) - \mu K_3 &= 0 \quad \mu \geq 0 \\ a(1-a)(\sigma(K_2) - q) + \mu K_2 &= 0 \end{aligned} \tag{2}$$

Proof in Appendix A.1.

A few notable observations:

- The regions of parameter space do *not* depend on a , but only on p, q, r . That is, the degree of information loss depends only on edge densities within and between the communities, not the size of the communities themselves.
- Most “real-world” graphs fall in the intermediate region Π_m : they have both sparsity and homophily, with within-group edges typically denser than between-group edges. It is rare to have strongly heterophilic communities (Π_s) or extremely-dense graphs (Π_d).
- From the embedding K , one can “read off” whether the embedding is invertible by checking the boundary conditions of each region: If $K_2^2 = K_1 K_3$, the original graph is in Π_d ; if $K = \mathbf{0}$, the original graph is in Π_s ; otherwise, Π_m .

4.2 Equivalence classes of graphs with identical embeddings lose density information

Theorem 1.3 tells us that, for an embedding K in the non-invertible region of parameter space Π_m , multiple graphons can map to K . How might these graphons be related? This is a key question: for example, attempting to predict the density of the graph would be hopeless if both very sparse and very dense graphs embed to the same representation K . Similarly, attempting to use the embeddings to do community clustering would be unrealistic if graphs with large majority groups and those with equal-sized communities both embed to the same representations.

In fact, we find that:

- Distinct graphons *do* in fact map to the same embedding.

- The embedding preserves the community structure. This follows from Thm 1: so long as $K_1 \neq K_3$ or $K_2 \neq K_3$, the block-constant matrix structure encodes the communities.
- Only some edge density information is preserved by the embedding; a given embedding represents an entire equivalence class of graphons.

In particular, each equivalence class consists of a linearly-related set of graphons, ranging from maximally dense communities (on the boundary of Π_d) to maximally sparse ones (when $q = 0$ or $q = 1$). This is quite a large range: the overall density of the graph is *not* encoded in the representation! That is, the embedding of a very sparse graph can “look identical to” the embedding of a very dense graph.

We explicitly characterize the equivalence classes induced by this embedding in Thm. 2.

Theorem 2 (Embedding-induced equivalence classes). *Partition Π_m into equivalence classes, where graphons $\mathcal{G} \sim \mathcal{G}'$ iff $K(\mathcal{G}) = K(\mathcal{G}')$. Fix any $\mathcal{G} = (p, q, r)$ and let $\hat{K} = K(\mathcal{G}) = (K_1, K_2, K_3)$. The equivalence class containing \mathcal{G} is*

$$F_{\hat{K}} = \left\{ (p, q, r) \in \Pi_m, \text{ where } \begin{array}{l} p = p_0 + \eta\Delta \\ q = q_0 + \mathbb{S}\Delta, \Delta \in \mathbb{R} \\ r = r_0 + \frac{1}{\eta}\Delta \end{array} \right\}, \quad (3)$$

where

$$\eta = \frac{1-a}{a} \sqrt{\frac{K_3}{K_1}} \quad \text{and} \quad \mathbb{S} = \begin{cases} +1 & q \leq 1/2 \\ -1 & q > 1/2 \end{cases}.$$

Equivalently, we can write the class as

$$F_{\hat{K}} = \left\{ \mathcal{G}' = \left(\begin{bmatrix} p & q \\ q & r \end{bmatrix} + \mathbb{S}\Delta \begin{bmatrix} \eta & 1 \\ 1 & 1/\eta \end{bmatrix} \right) : \mathcal{G}' \in \Pi_m, \Delta \in \mathbb{R} \right\}. \quad (4)$$

Proof in Appendix A.2.

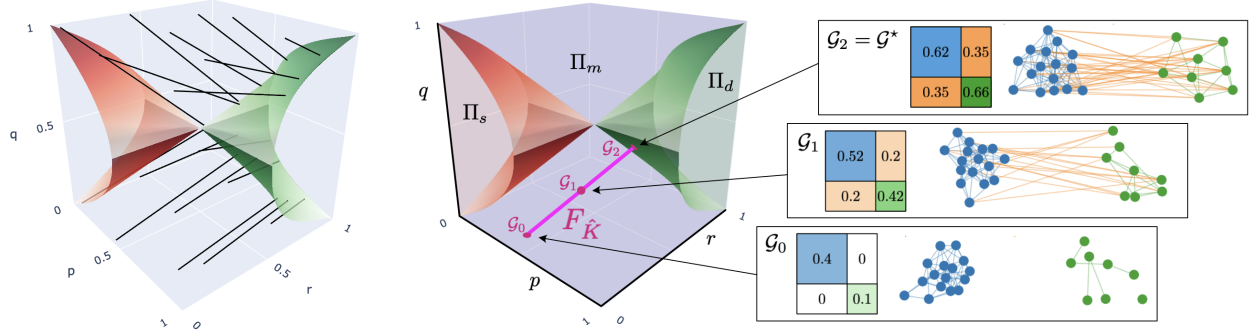
Graphons in the same equivalence class are *linearly related* in a particular way that depends on a “relative densifying parameter” η . The equivalence class corresponding to \hat{K} is a “line” of increasingly-dense graphons, in which p increases at rate η , r increases at rate $1/\eta$, and q increases at rate either 1 or -1 , depending on if $q \leq 1/2$ or not. A visualization of several of these linear equivalence classes is shown in Fig. 3a.

One example class is shown in Fig. 3b. Note that even the relative densities of the communities are not preserved by the embedding: in \mathcal{G}_0 , the larger (blue) community is denser, whereas in \mathcal{G}_2 the smaller (green) community is denser. In fact, we can exactly derive what the densest member of each equivalence class is:

Corollary 3. *For any graphon $\mathcal{G} \in \Pi_m$ with embedding $\hat{K} = (K_1, \pm\sqrt{K_1 K_3}, K_3)$, the densest graphon \mathcal{G}^* (in p, r) that has the same embedding is*

$$(p^*, q^*, r^*) \triangleq \arg \max_{\mathcal{G}' : K(\mathcal{G}') = K(\mathcal{G})} p' = (\sigma(K_1), \sigma(K_2), \sigma(K_3)).$$

This graphon (p^*, q^*, r^*) lies on the boundary between Π_m and Π_d .



(a) The equivalence classes of identically-embedded graphons are lines within Π_m . The slope of each line is controlled by the parameter η .

(b) An example of one such equivalence class, for the embedding $\hat{K} = (0.49, -0.59, 0.71)$ with $a = 0.66$, resulting in $\eta = 0.62$. All points along the $F_{\hat{K}}$ line have the same embedding, including graphons that are both maximally-dense (\mathcal{G}^* , on the boundary of Π_d) and maximally-sparse (\mathcal{G}_0).

Figure 3: Examples of equivalence classes in (p, q, r) space for $a = 0.66$.

It is easy to verify that this choice of (p^*, q^*, r^*) both matches the K values of Thm. 1.1 and satisfies Eq. 2 in Thm 1.3. Cor. 3 also allows us to restate $F_{\hat{K}}$ without relying on a prior-known (p_0, q_0, r_0) , by using (p^*, q^*, r^*) instead:

$$F_{\hat{K}} = \left\{ (p, q, r) \in \Pi_m, \text{ where } \begin{array}{l} p = \sigma(K_1) + \eta\Delta \\ q = \sigma(\mathbb{S}\sqrt{K_1 K_3}) + \mathbb{S}\Delta, \Delta \in \mathbb{R} \\ r = \sigma(K_3) + \frac{1}{\eta}\Delta \end{array} \right\} \quad (5)$$

5 Implications for downstream tasks

In general, embeddings are used as only a first step in doing some task of interest. Given the conditions on information loss and the equivalence classes of identically-embedded graphons we discuss above, what tasks can we gain theoretical insight on?

The equivalence classes described in Theorem 2 give reason to believe that using the embeddings alone for downstream tasks may not be sufficient, particularly in the non-invertible regime Π_m . Because a particular embedding K could come from a whole class of graphons, many downstream tasks may essentially boil down to “guessing” which graphon the embedding is from.

5.1 Community detection is robust except in Π_s

One common task is to do some form of classification or clustering of the nodes into communities. An easy consequence of Thm. 1 is that, in parameter regimes Π_m and Π_d , the community information (that is, which nodes are in which communities) is fully encoded in the loss-minimizing embedding; this information can be read off from the block-constant structure of K . Only in region Π_s is the community structure lost.

This is qualitatively similar to the Kesten-Stigum information-theoretic threshold [20], which describes conditions where SBM communities cannot be recovered from a *single instance* of the graph at rates better than chance. The KS threshold similarly implies that heterophilic communities

cannot be detected in certain cases, but detection scales with the size of the graph n (unlike our result, which is explicitly based on the graphon rather than a single instance).

Empirically, it is known that standard graph representation methods tend to do poorly on heterophilic graphs [21], and explicit algorithms for heterophilic graph learning tend to rely on somewhat specialized techniques; see [22]. The information loss that we show in Π_s gives additional theoretical justification for the poor performance of inner-product-based methods.

5.2 In Π_m , link prediction implicitly recovers a different graphon

Another common task is link prediction: given the embeddings $\{\omega_0, \omega_1, \dots\}$, output a probability for whether an edge exists between two nodes i and j .

A baseline algorithm predicts the densest graph possible. A baseline link-prediction algorithm for predicting edges using only the embeddings is as follows: compute the pairwise inner products between the embeddings, and then pass these scores through a sigmoid such as the σ , the standard logistic³. The predicted probability of edge (i, j) is

$$\sigma(\langle \omega_i, \omega_j \rangle) = \sigma(K[i, j]) = \begin{cases} \sigma(K_1) = p^* & \text{if } i, j \text{ in group 1} \\ \sigma(K_2) = q^* & \text{if } i, j \text{ in different groups} \\ \sigma(K_3) = r^* & \text{if } i, j \text{ in group 2} \end{cases}$$

That is, using this algorithm implicitly recovers the maximally-dense graphon $\mathcal{G}^* = (p^*, q^*, r^*)$ in the equivalence class (c.f. Cor. 3). If our original graph was sparse, this would be a very poor reconstruction!

On the other hand, knowing something as simple as the average degree of the graph would allow *perfect* graph reconstruction from the embedding: within each F_K , there's at most one graphon with a particular average degree. (See Prop. 6 in Appendix B.)

Of course, the task of link prediction is neither to compute a maximally-dense graph nor to reconstruct the original graph, but rather to predict some (typically small) fraction of additional edges that “should” be in the graph. A natural expectation of such a slightly-denser graph could be that it embed to the same representation⁴. This can be expressed as a normalized version of the baseline algorithm, which we discuss in Appendix B. **A reconstruction algorithm could reasonably recover any member of $F_{\hat{K}}$, depending on choice of normalization.**

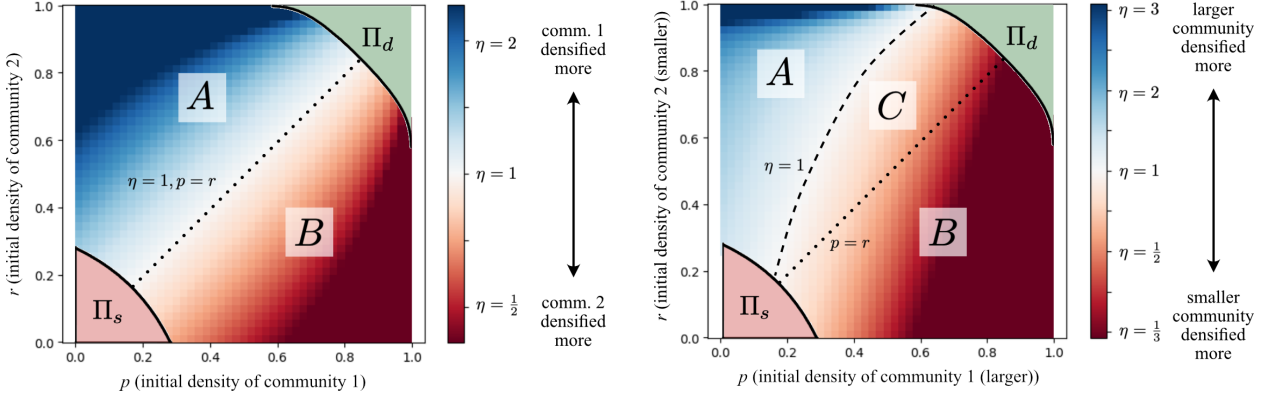
This example illustrates a general point about downstream tasks: by making algorithmic choices (e.g., choice of parameters, normalizations, assumptions, etc.), one is **implicitly choosing a “canonical” member among equivalently-embedded graphs**. We emphasize that this choice should be made thoughtfully and not in a data-agnostic way. In the simple link-prediction example we discuss, knowing the average degree (in addition to the embeddings) allows an exact recovery of the graphon, whereas relying on the embeddings alone fails.

5.2.1 Fairness; unbalanced densification

Substantial attention has been paid to whether network algorithms (such as link prediction) exacerbate or mitigate underlying biases in network structure (see [24] for an overview). It is standard to

³This method is used in variational graph auto-encoders [23] and is representative of a whole family of inner-product-based link prediction algorithms (e.g., [24, 25]).

⁴There are many plausible perspectives one could take on what link prediction should “do” [26]; we consider this representation-preserving objective because it directly illustrates consequences of our theoretical results.



(a) When the two communities are equal-sized ($a = 0.5$), link prediction strengthens the sparser community. In region A , community 1 is sparser ($p < r$) and is densified (because $\eta > 1$); the same is true for community 2 in region B .

(b) When the two communities are different sizes ($a = 0.75$), link prediction is also pushed towards strengthening smaller communities. In region C , this force “wins out” over the sparsity factor: community 2 (which is $\frac{1}{4}$ of the graph) is strengthened despite being denser.

Figure 4: Unbalanced densification in link prediction is affected by the relative sparsity and size of communities in the graph.

consider the density of a community as a measure of the “strength” or “power” of that community within a network [27]; so, depending on the context, it can be considered preferable to preferentially strengthen sparser and/or smaller communities [28], to equalize link probabilities relative to group membership [29, 30], or to reinforce between-community edges [31]⁵.

In our setting, a representation-preserving link-prediction algorithm densifies the communities at different rates: the larger community gains edges at rate η , while the smaller one gains edges at rate $\frac{1}{\eta}$. Based on η , we can characterize the set of graphons where different degrees of balanced/unbalanced densification occur: when $\eta > 1$, the larger community benefits, and when $\eta < 1$, the smaller community benefits. We plot the value of η against p and r for two different sets of community sizes in Fig. 4.

In Appendix C, we show that η is nearly monotonically increasing in r and nearly monotonically decreasing in p and a except at boundary points. That is, η varies with p, r, a as follows:

- The larger the difference in homophily between the groups $|p - r|$, the stronger the densifying effect (favoring the sparser community).
- The larger the difference in group size a , the stronger the densifying effect (favoring the smaller community).

There are areas of parameter space where these two are aligned (such as regions A and B in Fig. 4), and areas where they are in opposition (such as C in Fig. 4). In most of the parameter space, the sparser community is preferentially strengthened, *except* in the volume between the $\eta = 1$ and the $p = r$ surfaces, where the smaller, denser community is strengthened instead.

⁵This is often proposed in the context of polarization, although the empirical support for this is mixed [32, 33].

6 Discussion

The theoretical conditions we derive in this work allow us to draw connections between learned embeddings, information loss, and the structure of the graphon. Some of these connections have been empirically observed, and our results serve as a potential theoretical explanation; others are more novel, and we are excited to see whether they crop up in practice or become less pronounced under more complex models.

While the SBM graphon we study captures some aspects of real-world graphs (and their exchangeable nature makes them good candidates for theoretical analysis), there are many other properties (including, notably power-law degree distribution) that they do not capture. We expect that that our results can be generalized in multiple directions, including to more complex graphons and to more general generative models (e.g., graphexes [34]). Additionally, [9] characterize limiting distributions of loss-minimizing embeddings that use more complex sampling schemes (such as the random walks used by DeepWalk and node2vec); generalizing our results to these schemes is a direction for future work.

References

- [1] Bryan Perozzi, Rami Al-Rfou, and Steven Skiena. Deepwalk: Online learning of social representations. In *Proceedings of the 20th ACM SIGKDD international conference on Knowledge discovery and data mining*, pages 701–710, 2014.
- [2] Jian Tang, Meng Qu, Mingzhe Wang, Ming Zhang, Jun Yan, and Qiaozhu Mei. Line: Large-scale information network embedding. In *Proceedings of the 24th international conference on world wide web*, pages 1067–1077, 2015.
- [3] Aditya Grover and Jure Leskovec. node2vec: Scalable feature learning for networks. In *Proceedings of the 22nd ACM SIGKDD international conference on Knowledge discovery and data mining*, pages 855–864, 2016.
- [4] Jiezhong Qiu, Yuxiao Dong, Hao Ma, Jian Li, Kuansan Wang, and Jie Tang. Network embedding as matrix factorization: Unifying deepwalk, line, pte, and node2vec. In *Proceedings of the eleventh ACM international conference on web search and data mining*, pages 459–467, 2018.
- [5] Peng Cui, Xiao Wang, Jian Pei, and Wenwu Zhu. A survey on network embedding. *IEEE transactions on knowledge and data engineering*, 31(5):833–852, 2018.
- [6] C Seshadhri. Limitations of low dimensional graph embeddings. *Data Engineering*, page 94, 2023.
- [7] Comandur Seshadhri, Aneesh Sharma, Andrew Stolman, and Ashish Goel. The impossibility of low-rank representations for triangle-rich complex networks. *Proceedings of the National Academy of Sciences*, 117(11):5631–5637, 2020.
- [8] Szymon Snoeck, Noah Bergam, and Nakul Verma. Compressibility barriers to neighborhood-preserving data visualizations. *arXiv preprint arXiv:2508.07119*, 2025.

[9] Andrew Davison and Morgane Austern. Asymptotics of network embeddings learned via subsampling. *Journal of Machine Learning Research*, 24(138):1–120, 2023.

[10] Miller McPherson, Lynn Smith-Lovin, and James M Cook. Birds of a feather: Homophily in social networks. *Annual review of sociology*, 27(1):415–444, 2001.

[11] Sudhanshu Chanpuriya, Cameron Musco, Konstantinos Sotiropoulos, and Charalampos Tsourakakis. Deepwalking backwards: from embeddings back to graphs. In *International conference on machine learning*, pages 1473–1483. PMLR, 2021.

[12] Vikas Garg, Stefanie Jegelka, and Tommi Jaakkola. Generalization and representational limits of graph neural networks. In *International conference on machine learning*, pages 3419–3430. PMLR, 2020.

[13] László Lovász and Balázs Szegedy. Limits of dense graph sequences. *Journal of Combinatorial Theory, Series B*, 96(6):933–957, 2006.

[14] Peter Orbanz and Daniel M Roy. Bayesian models of graphs, arrays and other exchangeable random structures. *IEEE transactions on pattern analysis and machine intelligence*, 37(2):437–461, 2014.

[15] David J Aldous. Representations for partially exchangeable arrays of random variables. *Journal of Multivariate Analysis*, 11(4):581–598, 1981.

[16] Francesca Parise and Asuman Ozdaglar. Graphon games. In *Proceedings of the 2019 ACM Conference on Economics and Computation*, pages 457–458, 2019.

[17] Alexander Aurell, René Carmona, Gökçe Dayanikli, and Mathieu Lauriere. Finite state graphon games with applications to epidemics. *Dynamic Games and Applications*, 12(1):49–81, 2022.

[18] Paul W Holland, Kathryn Blackmond Laskey, and Samuel Leinhardt. Stochastic blockmodels: First steps. *Social networks*, 5(2):109–137, 1983.

[19] Krzysztof Nowicki and Tom A B Snijders. Estimation and prediction for stochastic blockstructures. *Journal of the American statistical association*, 96(455):1077–1087, 2001.

[20] Aurelien Decelle, Florent Krzakala, Cristopher Moore, and Lenka Zdeborová. Asymptotic analysis of the stochastic block model for modular networks and its algorithmic applications. *Physical Review E—Statistical, Nonlinear, and Soft Matter Physics*, 84(6):066106, 2011.

[21] Chao Gao, Zongming Ma, Anderson Y Zhang, and Harrison H Zhou. Community detection in degree-corrected block models. 2018.

[22] Sitao Luan, Chenqing Hua, Qincheng Lu, Liheng Ma, Lirong Wu, Xinyu Wang, Minkai Xu, Xiao-Wen Chang, Doina Precup, Rex Ying, et al. The heterophilic graph learning handbook: Benchmarks, models, theoretical analysis, applications and challenges. *arXiv preprint arXiv:2407.09618*, 2024.

[23] Thomas N Kipf and Max Welling. Variational graph auto-encoders. *arXiv preprint arXiv:1611.07308*, 2016.

- [24] Akrati Saxena, George Fletcher, and Mykola Pechenizkiy. Nodesim: node similarity based network embedding for diverse link prediction. *EPJ Data Science*, 11(1):24, 2022.
- [25] Daniele Malitesta, Alberto Carlo Maria Mancino, Pasquale Minervini, and Tommaso Di Noia. Dot product is all you need: Bridging the gap between item recommendation and link prediction. *arXiv preprint arXiv:2409.07433*, 2024.
- [26] Ajay Kumar, Shashank Sheshar Singh, Kuldeep Singh, and Bhaskar Biswas. Link prediction techniques, applications, and performance: A survey. *Physica A: Statistical Mechanics and its Applications*, 553:124289, 2020.
- [27] Linton C Freeman. Centrality in social networks conceptual clarification. *Social networks*, 1(3):215–239, 1978.
- [28] Ana-Andreea Stoica, Nelly Litvak, and Augustin Chaintreau. Fairness rising from the ranks: Hits and pagerank on homophilic networks. In *Proceedings of the ACM Web Conference 2024*, pages 2594–2602, 2024.
- [29] Yezi Liu, Hanning Chen, and Mohsen Imani. Promoting fairness in link prediction with graph enhancement. *Frontiers in Big Data*, 7:1489306, 2024.
- [30] Yanying Li, Xiuling Wang, Yue Ning, and Hui Wang. Fairlp: Towards fair link prediction on social network graphs. In *Proceedings of the international AAAI conference on web and social media*, volume 16, pages 628–639, 2022.
- [31] Michael Conover, Jacob Ratkiewicz, Matthew Francisco, Bruno Gonçalves, Filippo Menczer, and Alessandro Flammini. Political polarization on twitter. In *Proceedings of the international aaai conference on web and social media*, volume 5, pages 89–96, 2011.
- [32] Pranav Dandekar, Ashish Goel, and David T Lee. Biased assimilation, homophily, and the dynamics of polarization. *Proceedings of the National Academy of Sciences*, 110(15):5791–5796, 2013.
- [33] Eytan Bakshy, Solomon Messing, and Lada A Adamic. Exposure to ideologically diverse news and opinion on facebook. *Science*, 348(6239):1130–1132, 2015.
- [34] Victor Veitch and Daniel M Roy. The class of random graphs arising from exchangeable random measures. *arXiv preprint arXiv:1512.03099*, 2015.

A Proofs

A.1 Theorem 1: information loss regimes

Theorem 1 (Embedding Limit Regimes). *Suppose the graphon \mathcal{G} is a 2-block SBM($a, (p, q, r)$), and let ω_i be the embeddings learned by Algorithm 1 at convergence. Then, the inner product matrix of the embeddings $K(\mathcal{G}) \in \mathbb{R}^{n \times n}$ is a block-constant matrix:*

$$K(\mathcal{G}) = \begin{bmatrix} K_1 \mathbf{1}_{an \times an} & K_2 \mathbf{1}_{an \times (1-a)n} \\ K_2 \mathbf{1}_{(1-a)n \times an} & K_3 \mathbf{1}_{(1-a)n \times (1-a)n} \end{bmatrix},$$

where the values of $K_i \in \mathbb{R}$ depend on a, p, q, r as follows:

1. If $p, r \geq 1/2$ and $\sigma^{-1}(q)^2 < \sigma^{-1}(p)\sigma^{-1}(r)$, then $K_1 = \sigma^{-1}(p)$, $K_2 = \sigma^{-1}(q)$, $K_3 = \sigma^{-1}(r)$.
2. Otherwise, if $p, r \leq 1/2$ and $(1/2 - q)^2 \leq (1/2 - p)(1/2 - r)$, then $K_1 = K_2 = K_3 = 0$.
3. Otherwise,

$$K_2 = \begin{cases} -\sqrt{K_1 K_3} & \text{if } q \leq \frac{1}{2} \\ +\sqrt{K_1 K_3} & \text{if } q > \frac{1}{2} \end{cases},$$

with K_1, K_3 satisfying:

$$\begin{aligned} a^2(\sigma(K_1) - p) - \mu K_3 &= 0 \\ (1-a)^2(\sigma(K_3) - r) - \mu K_3 &= 0 \\ a(1-a)(\sigma(K_2) - q) + \mu K_2 &= 0 \end{aligned} \quad \mu \geq 0 \quad (2)$$

Proof. Let ρ be the sparsity parameter of the uniform vertex sampling, and our two-community SBM have parameters $(a, (p, q, r))$. Let K be the matrix of ERM-minimizing inner products (that is, $K_{i,j} = \langle \hat{\omega}_i, \hat{\omega}_j \rangle$). By Morgane's theorem, we know that K will converge to a positive definite block matrix

$$K = \begin{bmatrix} K_1 & K_2 \\ K_2 & K_3 \end{bmatrix}$$

where the block sizes are $an, (1-a)n$, corresponding to the sizes of the SBM communities. We're interested in the values of K_1, K_2, K_3 that minimize the empirical risk (Eq. 1):

$$\begin{aligned} \mathcal{R}_n(\omega_1, \dots, \omega_n) &= \sum_{i,j \in [n], i \neq j} \Pr((i, j) \in S(G_n) \mid G_n) \ell(\langle \omega_i, \omega_j \rangle, a_{ij}) \\ &= \frac{\rho}{n^2} \sum_{i \neq j} \ell(\langle \omega_i, \omega_j \rangle, a_{ij}) \end{aligned} \quad (\text{uniform vertex sampling})$$

Denoting the two SBM communities by A, B , we split the sum into cases:

$$\begin{aligned} &= \frac{\rho}{n^2} \left(\sum_{i,j \in A} \ell(\langle \omega_i, \omega_j \rangle, p) + \sum_{i,j \in B} \ell(\langle \omega_i, \omega_j \rangle, r) + 2 \sum_{i \in A, j \in B} \ell(\langle \omega_i, \omega_j \rangle, q) \right) \\ &= \rho (a^2 \ell(K_1, p) + (1-a)^2 \ell(K_3, r) + 2a(1-a) \ell(K_3, q)) \end{aligned}$$

The cross-entropy loss is

$$\begin{aligned}\ell(y, x) &= -x \log(\sigma(y)) - (1 - x) \log(1 - \sigma(y)) \quad \text{with } \sigma(y) = \frac{e^y}{1 + e^y} \\ &= \log(1 + e^y) - xy\end{aligned}$$

So, the problem of optimizing the risk \mathcal{R}_n is equivalent to minimizing the function

$$\mathcal{R}_n(K) = \rho \left(a^2(\log(1 + e^p) - K_1 p) + (1 - a)^2(\log(1 + e^r) - K_3 r) + 2a(1 - a)(\log(1 + e^q) - K_2 q) \right)$$

over positive definite matrices $K = [K_1, K_2; K_2, K_3]$. The positive definite constraint forces $K_1, K_3 \geq 0$ and $K_2^2 \leq K_1 K_3$. Letting $\mu_1, \mu_2, \mu_3 \geq 0$ be dual variables, the Lagrangian is $\mathcal{R}_n(K) - \mu_1 K_1 - \mu_2 K_3 - \mu_3 (K_1 K_3 - K_2^2)$. The KKT conditions for this problem state that any minima that satisfies the LICQ conditions must satisfy

$$a^2(\sigma(K_1) - p) - \mu_1 - K_3 \mu_3 = 0, \quad (1)$$

$$(1 - a)^2(\sigma(K_3) - r) - \mu_2 - K_1 \mu_3 = 0, \quad (2)$$

$$2a(1 - a)(\sigma(K_2) - q) + 2\mu_3 K_2 = 0, \quad (3)$$

$$\mu_1 K_1 = 0, \quad \mu_2 K_3 = 0, \quad \mu_3 (K_1 K_3 - K_2^2) = 0.$$

We now work case-by-case on which constraints are tight (i.e., whether μ_1, μ_2, μ_3 are zero). Each case is only feasible in a particular region of (p, q, r) parameter space; we show that the cases are feasible in regions of parameter space that are *disjoint* (except potentially at the boundaries). This allows us to conclude that the values of K that are taken in each case are the optimal ones.

Case 1: No constraints are tight (dense case). That is, $K_1 > 0, K_3 > 0, K_2^2 < K_1 K_3$. Then $\mu_1 = \mu_2 = \mu_3 = 0$. (1) reduces to $a^2(\sigma(K_1) - p) = 0 \implies K_1 = \sigma^{-1}(p)$. Similarly, $K_2 = \sigma^{-1}(q)$ and $K_3 = \sigma^{-1}(r)$. Since K_1, K_2, K_3 are positive, this exists only when $p > \frac{1}{2}, r > \frac{1}{2}$. The $K_2^2 < K_1 K_3$ constraint implies $\sigma^{-1}(q)^2 < \sigma^{-1}(p)\sigma^{-1}(r)$.

So, this case is feasible so long as $p > \frac{1}{2}, r > \frac{1}{2}$, and $\sigma^{-1}(q)^2 < \sigma^{-1}(p)\sigma^{-1}(r)$ and results in $K_1 = \sigma^{-1}(p), K_2 = \sigma^{-1}(q), K_3 = \sigma^{-1}(r)$.

Case 2: $K_2^2 \leq K_1 K_3$ is tight, and the other constraints are loose (middle case). So, $K_1 > 0, K_3 > 0$; these imply $\mu_1 = \mu_2 = 0$ and $\mu_3 \geq 0$. Here, we split further into two cases:

Case 2(a): $K_2 = -\sqrt{K_1 K_3}, K_1 > 0, K_3 > 0$ (sparse cross-edges). The KKT conditions become:

$$a^2(\sigma(K_1) - p) - K_3 \mu_3 = 0, \quad (4)$$

$$(1 - a)^2(\sigma(K_3) - r) - K_1 \mu_3 = 0, \quad (5)$$

$$2a(1 - a)(\sigma(-\sqrt{K_1 K_3}) - q) - 2\mu_3 \sqrt{K_1 K_3} = 0, \quad (6)$$

The first equation implies $a^2(\sigma(K_1) - p) \geq 0 \implies \sigma(K_1) \geq p$. Combined with the constraint that $K_1 \geq 0$, then $K_1 \geq \max(0, \sigma^{-1}(p))$. Similarly, $K_3 \geq \max(0, \sigma^{-1}(r))$; so, $\sqrt{K_1 K_3} \geq \sqrt{\max(0, \sigma^{-1}(p)) \max(0, \sigma^{-1}(r))}$.

Rearranging the third equation, we know

$$\sigma(-\sqrt{K_1 K_3}) - q = \frac{\mu_3}{a(1 - a)} \sqrt{K_1 K_3} \geq 0$$

So $\sigma(-\sqrt{K_1 K_3}) \geq q$, which implies $\sqrt{K_1 K_3} \leq -\sigma^{-1}(q)$.

Since $\sqrt{K_1 K_3} > 0$, this is only feasible when $-\sigma^{-1}(q) > 0$, so $q < \frac{1}{2}$.

Finally, we combine the bounds on $\sqrt{K_1 K_3}$:

$$\begin{aligned} \sqrt{\max(0, \sigma^{-1}(p)) \max(0, \sigma^{-1}(r))} &\leq \sqrt{K_1 K_3} \leq -\sigma^{-1}(q) \\ \implies \sigma^{-1}(q)^2 &\geq \max(0, \sigma^{-1}(p)) \max(0, \sigma^{-1}(r)) \\ \implies \sigma^{-1}(q)^2 &\geq \sigma^{-1}(p)\sigma^{-1}(r) \text{ or } p \leq \frac{1}{2} \text{ or } r \leq \frac{1}{2} \end{aligned}$$

So this case ($K_2 = -\sqrt{K_1 K_3}, K_1 > 0, K_3 > 0$) is feasible so long as $q < \frac{1}{2}$ and $(\sigma^{-1}(q)^2 \geq \sigma^{-1}(p)\sigma^{-1}(r) \text{ or } p \leq \frac{1}{2} \text{ or } r \leq \frac{1}{2})$.

Case 2(b): $K_2 = +\sqrt{K_1 K_3}, K_1 > 0, K_3 > 0$ (**dense cross-edges**). This case is very similar to case 2(a): $\sqrt{K_1 K_3} \geq \sqrt{\max(0, \sigma^{-1}(p)) \max(0, \sigma^{-1}(r))}$. However, the sign changes means that $\sqrt{K_1 K_3} \leq \sigma^{-1}(q)$, which implies $q < \frac{1}{2}$.

Squaring both sides as before, we obtain the same condition:

$$\sigma^{-1}(q)^2 \geq \sigma^{-1}(p)\sigma^{-1}(r) \text{ or } p \leq \frac{1}{2} \text{ or } r \leq \frac{1}{2}$$

So this case ($K_2 = +\sqrt{K_1 K_3}, K_1 > 0, K_3 > 0$) is feasible so long as $q > \frac{1}{2}$ and $(\sigma^{-1}(q)^2 \geq \sigma^{-1}(p)\sigma^{-1}(r) \text{ or } p \leq \frac{1}{2} \text{ or } r \leq \frac{1}{2})$.

Case 3: $K_1 = 0$ or $K_3 = 0$ or both (edge cases). In all of these cases, the PSD constraint $K_2^2 \leq K_1 K_3$ forces $K_2 = 0$. Then, the third KKT condition $(a(1-a)(\sigma(0) - q) - 2\mu_3(0) = 0)$ forces $q = \frac{1}{2}$.

- When $K_1 = 0, K_3 \neq 0$, then $\mu_2 = 0$. The first KKT condition $\mu_1 \geq 0$ forces $a^2(\sigma(0) - p) \geq 0$, that is, $\frac{1}{2} \geq p$. The second KKT condition becomes $(1-a)^2(\sigma(K_3) - r) - 0 - 0\mu_3$, which is satisfied only when $K_3 = \sigma^{-1}(r)$. So, the feasible region is $q = \frac{1}{2}, p \leq \frac{1}{2}, r > \frac{1}{2}$.
- Similarly, when $K_3 = 0, K_1 \neq 0$, the second KKT condition forces $\frac{1}{2} \geq r$, and the first KKT condition forces $K_1 = \sigma^{-1}(p)$. So, the feasible region is $q = \frac{1}{2}, r \leq \frac{1}{2}, p > \frac{1}{2}$.
- When both $K_1 = K_3 = 0$, then the feasible region is $q = \frac{1}{2}, p \leq \frac{1}{2}$ and $r \leq \frac{1}{2}$.

Non-KKT cases. Finally, we check points that *don't* satisfy the linear independence constraint qualification (LICQ) conditions, i.e., potential solutions that would not be found by KKT. Our constraints are $K_1 \geq 0, K_3 \geq 0, K_1 K_3 - K_2^2 \geq 0$. Their gradients are $(1, 0, 0), (0, 0, 1)$, and $(K_3, -2K_2, K_1)$ respectively. These gradients are linearly independent at all points except for $(0, 0, 0)$ (the origin) and $(0, 0, K_3)$ and $(K_1, 0, 0)$. We check the optimality of these points first:

- $(0, 0, 0)$ is globally optimal iff the directional derivative in every feasible direction is nonnegative. That is, for all feasible (u, v, w) in the feasible cone (that is, $u \geq 0, w \geq 0, v^2 \leq uw$),

$$\nabla \mathcal{R}_n(0, 0, 0) \cdot (u, v, w) \geq 0.$$

$\nabla \mathcal{R}_n(0, 0, 0)$ is $(a^2(1/2-p), 2a(1-a)(1/2-q), (1-a)^2(1/2-r))$. Letting $u = x^2, w = z^2, v = \rho xz$ for $x \geq 0, z \geq 0, |\rho| \leq 1$ (which ensures the constraints are satisfied), this is

$$\nabla \mathcal{R}_n(0, 0, 0) \cdot (u, v, w) = \left(\frac{1}{2} - p\right)(ax)^2 + 2\left(\frac{1}{2} - q\right)\rho(ax)(1-a)z + \left(\frac{1}{2} - r\right)((1-a)z)^2 \geq 0$$

This is minimized by having $\rho = \text{sign}(1/2 - q)$. Rearranging and letting $t = \frac{ax}{(1-a)z}$, this is

$$\frac{1}{(1-a)^2 z^2} \left(\frac{1}{2} - p \right) t^2 + 2 \left| \frac{1}{2} - q \right| t + \left(\frac{1}{2} - r \right) \geq 0$$

which holds whenever $\frac{1}{2} - p \geq 0$, $\frac{1}{2} - r \geq 0$, and $(\frac{1}{2} - q)^2 \leq (\frac{1}{2} - p)(\frac{1}{2} - r)$.

That is, when $p \leq \frac{1}{2}$, $r \leq \frac{1}{2}$, and $(\frac{1}{2} - q)^2 \leq (\frac{1}{2} - p)(\frac{1}{2} - r)$, the risk is minimized by letting $K_1 = K_2 = K_3 = 0$.

- $(K_1, 0, 0)$ is feasible along the curve $\gamma(t) = (K_1, t, t^2/K_1)$ for $t \in \mathbb{R}$. The directional derivative along γ at $t = 0$ is

$$\frac{d}{dt} \mathbb{R}_n(\gamma(t))|_{t=0} = 2a(1-a)(1/2 - q).$$

This is only minimizing at $q = \frac{1}{2}$. This becomes identical to case 3 in the KKT cases.

- $(0, 0, K_3)$ is similarly identical to case 3 of the KKT cases.

These are the only cases where a non-KKT case can be optimal. Since the cases are feasible in disjoint regions of parameter space, the theorem is proved. \square

A.2 Theorem 2: Equivalence Classes in Π_m

Theorem 2 (Embedding-induced equivalence classes). *Partition Π_m into equivalence classes, where graphons $\mathcal{G} \sim \mathcal{G}'$ iff $K(\mathcal{G}) = K(\mathcal{G}')$. Fix any $\mathcal{G} = (p, q, r)$ and let $\hat{K} = K(\mathcal{G}) = (K_1, K_2, K_3)$. The equivalence class containing \mathcal{G} is*

$$F_{\hat{K}} = \left\{ (p, q, r) \in \Pi_m, \text{ where } \begin{array}{l} p = p_0 + \eta\Delta \\ q = q_0 + \mathbb{S}\Delta, \Delta \in \mathbb{R} \\ r = r_0 + \frac{1}{\eta}\Delta \end{array} \right\}, \quad (3)$$

where

$$\eta = \frac{1-a}{a} \sqrt{\frac{K_3}{K_1}} \quad \text{and} \quad \mathbb{S} = \begin{cases} +1 & q \leq 1/2 \\ -1 & q > 1/2 \end{cases}.$$

Equivalently, we can write the class as

$$F_{\hat{K}} = \left\{ \mathcal{G}' = \left(\begin{bmatrix} p & q \\ q & r \end{bmatrix} + \mathbb{S}\Delta \begin{bmatrix} \eta & 1 \\ 1 & 1/\eta \end{bmatrix} \right) : \mathcal{G}' \in \Pi_m, \Delta \in \mathbb{R} \right\}. \quad (4)$$

Proof. We recall the KKT-derived conditions from Theorem 1 (case 3):

$$\begin{aligned} a^2(\sigma(K_1) - p) - \mu K_3 &= 0 \\ (1-a)^2(\sigma(K_3) - r) - \mu K_1 &= 0 \quad \mu \geq 0 \\ a(1-a)(\sigma(K_2) - q) + \mu K_2 &= 0 \end{aligned} \quad (2)$$

Fix K_1, K_3 . In this case,

$$K_2 = \begin{cases} -\sqrt{K_1 K_3} & q \leq \frac{1}{2} \\ +\sqrt{K_1 K_3} & q > \frac{1}{2} \end{cases} = \mathbb{S} \sqrt{K_1 K_3} \quad \text{where } \mathbb{S} = \begin{cases} 1 & q \leq \frac{1}{2} \\ -1 & q > \frac{1}{2} \end{cases}$$

Suppose both (p_0, q_0, r_0) and (p_0+x, q_0+y, r_0+z) have the same embedding $\hat{K} = (K_1, \mathbb{S}K_2, K_3)$: that is, they result in solutions to (2) of (K_1, K_3, μ) and (K_1, K_3, μ') respectively. Then

$$\begin{aligned} a^2(\sigma(K_1) - (p_0 + x)) - \mu' K_3 &= a^2(\sigma(K_1) - p_0) - \mu K_3 = 0 \\ \implies -a^2 x - \mu' K_3 &= \mu K_3 \\ \implies x &= (\mu - \mu') \frac{K_3}{a^2} \end{aligned}$$

Similarly,

$$y = (\mu - \mu') \frac{\mathbb{S}\sqrt{K_1 K_3}}{a(1-a)} \quad \text{and} \quad z = (\mu - \mu') \frac{K_1}{(1-a)^2}$$

So,

$$x = y \cdot \mathbb{S} \frac{1-a}{a} \sqrt{\frac{K_3}{K_1}} \quad \text{and} \quad z = y \cdot \mathbb{S} \frac{a}{1-a} \sqrt{\frac{K_1}{K_3}}$$

Since μ' is free, the class is simply $\{(p_0 + x, q_0 + y, z_0 + z) : \mu' \in \mathbb{R}\} \cap \Pi_m$. Letting $\eta = \frac{1-a}{a} \sqrt{\frac{K_3}{K_1}}$ and reparametrizing $\mathbb{S}y(\mu - \mu') = \Delta$, the class becomes

$$F_{\hat{K}} = \left\{ (p, q, r) \in \Pi_m, \text{ where } \begin{array}{l} p = p_0 + \eta \Delta \\ q = q_0 + \mathbb{S} \Delta, \Delta \in \mathbb{R} \\ r = r_0 + \frac{1}{\eta} \Delta \end{array} \right\}, \quad (6)$$

□

Observation 4. *We can also express*

$$\eta = \sqrt{\frac{\sigma(K_1) - p}{\sigma(K_3) - r}}.$$

This can be useful to avoid numerical issues with $\sqrt{\frac{K_1}{K_3}}$ when K_1 or K_3 are near 0, and also gives some intuition for an alternative interpretation of η : as a ratio of the amount of “forced error” between $\sigma(K_1)$ and p and between $\sigma(K_3)$ and r .

Proof. Rewriting the first two KKT conditions,

$$\mu K_3 = a^2(\sigma(K_1) - p) \quad \mu K_1 = (1-a)^2(\sigma(K_3) - r)$$

Dividing these two equations:

$$\frac{\mu K_3}{\mu K_1} = \frac{a^2(\sigma(K_1) - p)}{(1-a)^2(\sigma(K_3) - r)}$$

So,

$$\eta = \frac{1-a}{a} \sqrt{\frac{K_1}{K_3}} = \frac{1-a}{a} \sqrt{\frac{a^2(\sigma(K_1) - p)}{(1-a)^2(\sigma(K_3) - r)}} = \sqrt{\frac{\sigma(K_1) - p}{\sigma(K_3) - r}}$$

□

B Graph reconstruction, normalized link prediction

B.1 Link prediction

We briefly discuss the simple link-prediction algorithm we outline in Section 5.2: for each pair of nodes (i, j) , predict the edge with probability $\pi_{i,j} = \sigma(\langle \omega_i, \omega_j \rangle)$, where ω_i is the learned embedding for node i and $z \in [0, 1]$ is a normalizing factor.

In a sense, this is both a link-prediction and a graph(on)-recovery algorithm: you could use it to add edges to a sampled graph $G \sim \mathcal{G}$, or you could use it to come up with a new graphon \mathcal{G}' that embeds to the same representation as \mathcal{G} . We restrict ourselves to the “partial information” regime of graphons in Π_m , where a family of graphons $F_{\hat{K}}$ all map to the same embedding \hat{K} .

Proposition 5. *This algorithm recovers the maximally-dense graphon \mathcal{G}^* of the family $F_{\hat{K}}$.*

As we state in the Section 5.2, this follows from the structure of K in regime Π_m :

$$\sigma(\langle \omega_i, \omega_j \rangle) = \sigma(K[i, j]) = \begin{cases} \sigma(K_1) = p^* & \text{if } i, j \text{ in group 1} \\ \sigma(K_2) = q^* & \text{if } i, j \text{ in different groups} \\ \sigma(K_3) = r^* & \text{if } i, j \text{ in group 2} \end{cases}$$

In addition, one could consider a “normalized” or “rescaled” version of this algorithm that interpolates the edges between the original graphon \mathcal{G} and the baseline \mathcal{G}^* . A linear interpolation recovers the class $F_{\hat{K}} \cap ([p_0, p^*] \times [q_0, q^*] \times [r_0, r^*])$.

Generalizing further, a “graph reconstruction” view on the task could also plausibly “rescale” to something sparser than the original graph, recovering the entire $F_{\hat{K}}$.

B.2 Exact recovery from embedding using density

Proposition 6. *For a given $\hat{K} \neq \mathbf{0}$, no two $\mathcal{G}, \mathcal{G}' \in F_{\hat{K}}$ have the same average degree (or, equivalently, edge density).*

This follows directly because $F_{\hat{K}}$ is linear; each element of $F_{\hat{K}}$ is uniquely defined by its value of Δ , the average degree is linear in Δ :

$$\begin{aligned} \text{average degree} &= \frac{1}{n} \sum_v \mathbb{E}[\deg(v)] \\ &= \frac{1}{n} \left(a^2(p_0 + \Delta\eta) + a(1-a)(q_0 + \Delta) + (1-a)^2(r_0 + \frac{\Delta}{\eta}) \right) \\ &= \frac{1}{n} (a^2 p_0 + a(1-a)q_0 + (1-a)^2 r_0) + \frac{1}{n} (a^2 \eta a (1-a) + (1-a)^2 / \eta) \Delta \end{aligned}$$

So, knowing the average degree suffices for perfect recovery of the graphon.

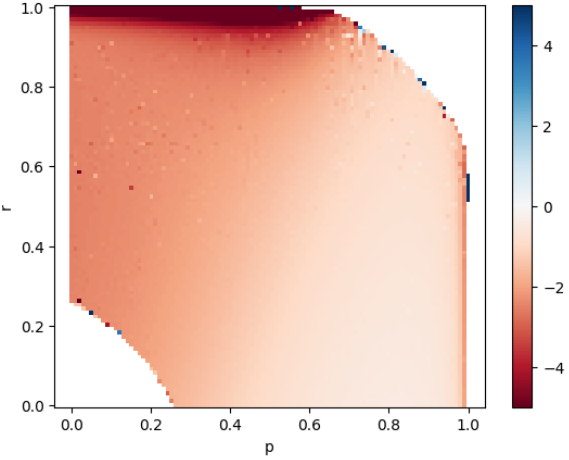
C Scaling of η with graphon parameters (a, p, q, r)

In most regions of parameter space, η ’s slope depends on a, p, q, r as follows:

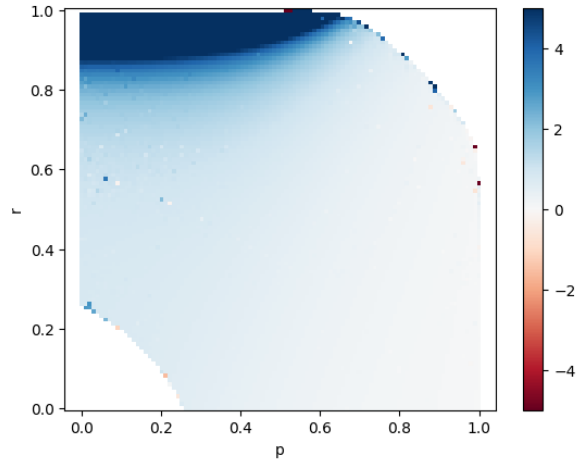
- η decreases with a (which preferentially strengthens the smaller community, with a larger effect the smaller the community is)

- η decreases with p (which preferentially strengthens the sparser community).
- η increases with r (which also preferentially strengthens the sparser community).

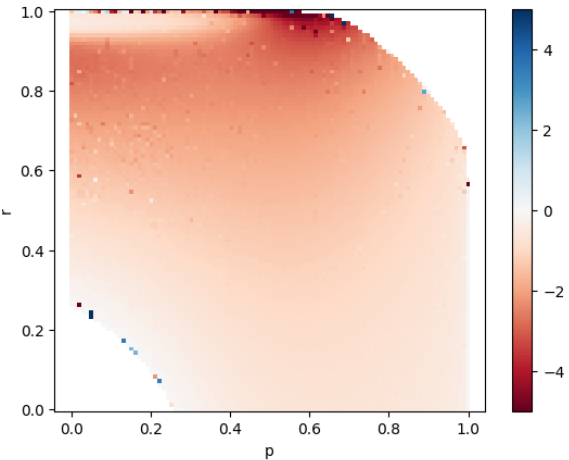
This is easiest to verify numerically, by computing the partial derivative of η at different points in Π_m , shown in Fig. 5.



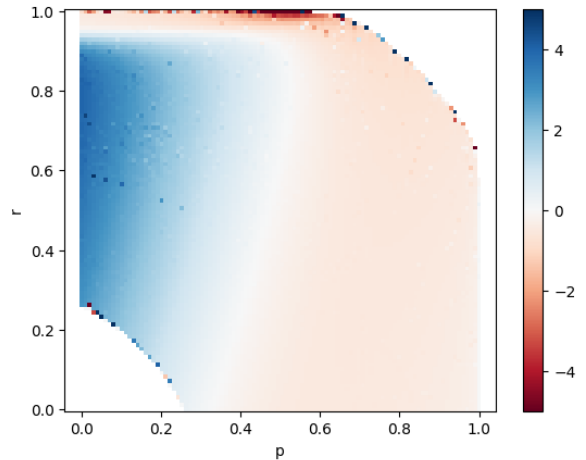
(a) $\frac{\partial\eta}{\partial p}$ is negative at all but a few boundary points.



(b) $\frac{\partial\eta}{\partial r}$ is positive at all but a few boundary points.



(c) $\frac{\partial\eta}{\partial a}$ is negative at all but a few boundary points.



(d) η is not monotonic in q : $\frac{\partial\eta}{\partial r}$ changes sign depending on parameters.

Figure 5: Partial derivatives of η with respect to parameters p, q, r, a at $a = 0.55, q = 0.15$. η is nearly monotonic in p, r (strengthening the sparser community), and a (strengthening the smaller community), but not monotonic in q .